

Towards an efficient simulation framework for plasmonic organic hybrid E/O modulators

Alberto Tibaldi^{*†}, Mohammadamin Ghomashi^{*}, Francesco Bertazzi^{*†}, Marco Vallone^{*},
Michele Goano^{*†}, and Giovanni Ghione^{*}

^{*} Department of Electronics and Telecommunications, Politecnico di Torino, 10129 Turin, Italy

[†] CNR-IEIIT c/o Politecnico di Torino, 10129 Turin, Italy

E-mail: alberto.tibaldi@polito.it

Abstract—Due to the large computational resources required, with CPU times of the order of several days, full-wave optical simulators can be hardly exploited for the modeling and optimization of plasmonic organic hybrid electro/optic modulators. With the aim to drastically reduce such complexity, in this work we present a *divide-et-impera* strategy reducing the number of FDTD simulations required to perform a full-wave simulation of the modulation response. This framework is demonstrated on 2D simulations of a device inspired by the literature, tracing a viable roadmap towards a computationally sustainable, yet accurate, comprehensive 3D simulation framework.

I. INTRODUCTION

In silicon photonics, plasmonic organic hybrid (POH) electro-optic (E/O) Mach-Zehnder (MZ) modulators are among the most appealing innovative solutions for chip-to-chip and datacenter-level communications at $1.3\ \mu\text{m}$ and $1.55\ \mu\text{m}$ wavelengths [1], for their unique potential for integration at chip scales, fJ/bit power consumption, Pb/s channel capacity, almost unlimited speed and exceptional E/O material characteristics [2].

POH modulators exploit polymer-based E/O materials consisting of chromophore molecules dispersed in a polymer host medium, which are oriented according to a static poling electric field [3]. Modulation of the material refractive index is obtained by an RF electric field applied to the poled material. This material fills the phase shifter slots, which are designed to support plasmonic modes. Thanks to the nanometer widths, very large RF electric fields can be obtained with low applied voltages, thus enhancing the E/O effect and allowing to keep the modulator length in the micrometer range.

From this description, one understands that simulating the static modulator response, which provides important figures of merit such as the ON-OFF voltage V_π , the insertion loss L_I and the extinction ratio R_E , needs a multiphysics treatment. In fact, evaluating the E/O modulation requires a model of the local RF electric field [4], that is then used to obtain a complex, position-dependent, anisotropic refractive index profile. This, in turn, is provided as input of the full-wave optical model. As a first approximation, one could approximate the RF electric field in the plasmonic waveguide as constant in the slot and orthogonal to the walls [2, eq. (1)]. Even accepting these simplifications, an optical model overcoming mode simulations [5] coupled to simple system-level formulas [6, Sec. 6.4.2] requires a full-wave simulation, for instance

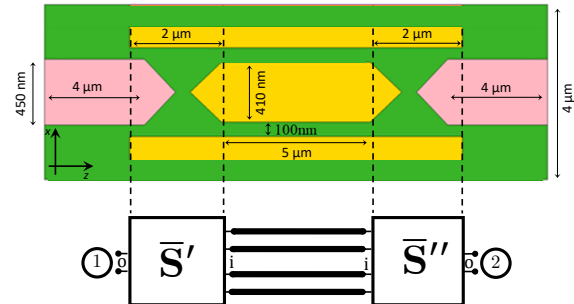


Fig. 1. Top: geometry of the device under test. Bottom: schematic representation of the *divide-et-impera* approach.

with the finite-difference time-domain (FDTD) method, for each RF voltage V_{RF} , leading to a formidable computational burden.

The scope of this work is to reduce the complexity of the optical problem, yet remaining in the framework of full-wave electromagnetic simulations, through a *divide-et-impera* strategy. This approach is presented and applied to a reference POH E/O MZ modulator inspired to literature data [7], comparing the results with the ones obtained simulating the entire device (*all-in-one* simulation).

II. DIVIDE-ET-IMPERA APPROACH AND RESULTS

The device under study is sketched in Fig.1(top). The picture is not to scale. The operating wavelength is $1.55\ \mu\text{m}$. The DLD-164 polymer ($n_{\text{E/O}} = 1.83$) [1], [3] used as E/O material is in green. The input signal is brought by the left Si waveguide ($n_{\text{Si}} = 3.6$), 450 nm thick; it can be seen that the output section of the modulator exhibits the same configuration. The two $5\ \mu\text{m}$ long arms of the MZ modulators are the plasmonic slab waveguides, 100 nm wide, between the gold central island (410 nm wide) and horizontal rails ($n_{\text{Au}} = 0.2524 + j10.4386$). The $2\ \mu\text{m}$ long splitter (left) and recombiner (right) convert the dielectric mode into the plasmonic modes of the slab waveguides and viceversa. Focusing on the splitter, this consists of a taper of the dielectric waveguide in front of a taper of the gold island. The refractive index change induced by the E/O effect is included only in the plasmonic slabs, where the optical–RF fields interaction is maximum.

Assuming that only the fundamental TM mode is propagating in the dielectric waveguides, we compute the static modulator response as the transmission coefficient quantifying the power of the input waveguide mode transferred into the output waveguide mode, reported with a solid blue curve in Fig. 2. This result has been obtained from FDTD simulations of the device sketched in Fig. 1, launching the mode of the left Si waveguide as input field and computing the mode amplitude of the field at the output waveguide through an S-parameter sweep [8]. The simulations have been performed in 2D, translationally invariant with respect to y , and with a uniform 10 nm mesh step.

The insertion loss L_I have been estimated to be 2.88 dB, which is compatible with the experimental results in [7]. Instead, the ON-OFF voltage has been estimated to $V_\pi = 12$ V, which is larger than the measure (10 V). This overestimation could be ascribed to the underestimation of the E/O effect related to the RF field approximation. 3D effects could also impact on V_π , as well as on the extinction ratio, which as been estimated to be quite large ($R_E = 29.35$ dB).

The solid blue curve has been obtained from the full-wave simulations of the entire device, performed at each RF voltage. Even though this is still possible with 2D simulations, this would lead to the need of large computational times and resources in 3D. An alternative approach could be formulated considering that in the most critical sections from the simulation perspective, the splitter and recombiner, the E/O effect is neglected, making them voltage-independent. Starting from this observation, the *divide-et-impera* approach described in the bottom section of Fig. 1 has been conceived. This is based on computing with FDTD only the 3×3 scattering matrix of the splitter, where the scattering parameters of the left port are related to the dielectric mode expansion coefficients, while those of the right ports to the excitation of the plasmonic modes (the elements of the recombiner S-matrix are identical, just ordered in the matrix differently). Then, a modal simulation providing the (plasmonic) transmission line refractive indexes n_{eff} is performed for some input RF voltages: being $n_{\text{eff}}(V_{\text{RF}})$ almost linear, it can be interpolated accurately. Finally, the entire device can be treated as a bimodal Fabry-Pérot interferometer, computing the static modulation response with the cascade formulas [9], [10], which are also valid in presence of losses [11]. The results of this *divide-et-impera* approach are reported in the dashed red line of Fig. 2, which overlaps almost perfectly with its *all-in-one* counterpart (except for small deviations, at about -30 dB levels).

It is to be remarked that obtaining this result requires only modal simulations of the plasmonic slots, a single ($V_{\text{RF}} = 0$ V) FDTD simulation of the splitter, and simple cascade formulas. In this work, the *divide-et-impera* approach has been demonstrated on 2D simulations of POH devices. However, it can be extended to 3D geometries with a few adjustments, promising to open the door towards the realistic comprehensive simulation of large modulators, also with other material systems/configurations.

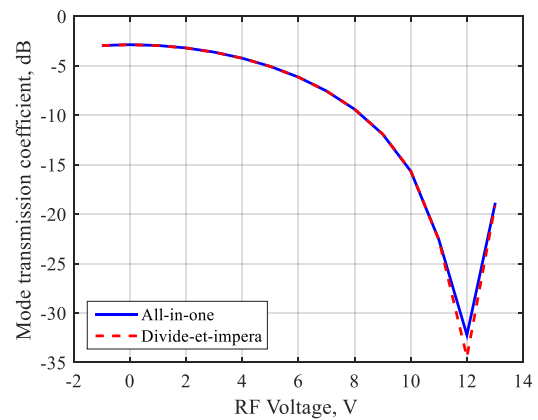


Fig. 2. Static modulation response of the device sketched in Fig. 1(top), obtained simulating the entire device (*all-in-one* model, solid blue curve) and with the *divide-et-impera* approach (dashed red curve).

ACKNOWLEDGMENTS

Support from the project HIRPO2017030805 “Modelling of integrated Mach-Zehnder electro-optic modulators: from materials to system-level design” of HiSilicon is gratefully acknowledged.

REFERENCES

- [1] W. Heni, Y. Fedoryshyn, B. Baeuerle, *et al.*, “Plasmonic IQ modulators with attojoule per bit electrical energy consumption,” *Nature Commun.*, vol. 10, p. 1694, Appl. Phys. Rev. 2019.
- [2] C. Haffner, W. Heni, Y. Fedoryshyn, *et al.*, “Plasmonic organic hybrid modulators—scaling highest speed photonics to the microscale,” *Proc. IEEE*, vol. 104, no. 12, pp. 2362–2379, Dec. 2016.
- [3] D. L. Elder, S. J. Benight, J. Song, *et al.*, “Matrix-assisted poling of monolithic bridge-disubstituted organic NLO chromophores,” *Chem. Mater.*, vol. 26, no. 2, pp. 872–874, Jan. 2014.
- [4] F. Bertazzi, G. Ghione, and M. Goano, “Efficient quasi-TEM frequency-dependent analysis of lossy multiconductor lines through a fast reduced-order FEM model,” *IEEE Trans. Microwave Theory Tech.*, vol. MTT-51, no. 9, pp. 2029–2035, Sept. 2003.
- [5] F. Bertazzi, O. A. Peverini, M. Goano, *et al.*, “A fast reduced-order model for the full-wave FEM analysis of lossy inhomogeneous anisotropic waveguides,” *IEEE Trans. Microwave Theory Tech.*, vol. MTT-50, no. 9, pp. 2108–2114, Sept. 2002.
- [6] G. Ghione, *Semiconductor Devices for High-Speed Optoelectronics*. Cambridge, U.K.: Cambridge University Press, 2009.
- [7] C. Haffner, W. Heni, Y. Fedoryshyn, *et al.*, “All-plasmonic Mach-Zehnder modulator enabling optical high-speed communication at the microscale,” *Nature Photon.*, vol. 9, pp. 525–528, July 2015.
- [8] Lumerical Inc., 2019. [Online]. Available: <https://www.lumerical.com/products/>
- [9] R. Orta, A. Tibaldi, and P. Debernardi, “Bimodal resonance phenomena—part I: generalized Fabry-Pérot interferometers,” *IEEE J. Quantum Electron.*, vol. 52, no. 12, pp. 6 100 508–1–8, 2016.
- [10] R. Orta, A. Tibaldi, and P. Debernardi, “Bimodal resonance phenomena—part II: high/low-contrast grating resonators,” *IEEE J. Quantum Electron.*, vol. 52, no. 12, pp. 6 600 409–1–8, 2016.
- [11] A. Tibaldi, P. Debernardi, and R. Orta, “Bimodal resonance phenomena—part III: high-contrast grating reflectors,” *IEEE J. Quantum Electron.*, vol. 54, no. 6, pp. 6 600 108–1–8, 2018.